Nucleic Acids Research, 2005, Vol. 33, No. 18 ***e164***
doi:10.1093/nar/gni165

Partial ^{13}C isotopic enrichment of nucleoside monophosphates: useful reporters for NMR structural studies

Anita I. Kishore, Michael R. Mayer and James H. Prestegard*

Complex Carbohydrate Research Center, University of Georgia, Athens, GA 30602-4712, USA

Received August 29, 2005; Revised and Accepted October 3, 2005

ABSTRACT

Analysis of the ^{13}C isotopic labeling patterns of nucleoside monophosphates (NMPs) extracted from *Escherichia coli* grown in a mixture of C-1 and C-2 glucose is presented. By comparing our results to previous observations on amino acids grown in similar media, we have been able to rationalize the labeling pattern based on the well-known biochemistry of nucleotide biosynthesis. Except for a few notable absences of label (C4 in purines and C3′ in ribose) and one highly enriched site (C1′ in ribose), most carbons are randomly enriched at a low level (an average of 13%). These sparsely labeled NMPs give less complex NMR spectra than their fully isotopically labeled analogs due to the elimination of most ^{13}C–^{13}C scalar couplings. The spectral simplicity is particularly advantageous when working in ordered systems, as illustrated with guanosine diphosphate (GDP) bound to ADP ribosylation factor 1 (ARF1) aligned in a liquid crystalline medium. In this system, the absence of scalar couplings and additional long-range dipolar couplings significantly enhances signal to noise and resolution.

INTRODUCTION

The use of uniform, isotopic enrichment in biological molecules has been indispensable to the advancement of biomolecular NMR. Resonance assignment of ^{13}C and ^{15}N nuclei in proteins up to 40 kDa and nucleic acids up to 15 kDa is now routine in high resolution NMR (1–3). In solid-state NMR and in NMR of partially ordered systems, isotope labeling methods are also advantageous. In general, uniform isotopic labeling has facilitated assignment but has introduced some unique spectroscopic problems as well. For example, abundant scalar and dipolar couplings of adjacent ^{13}C nuclei, actually degrade resolution and can lead to dilution of signal by transfer of magnetization through multiple pathways. Selective labeling reduces the probability of adjacent ^{13}C groups, improving spectral resolution and simplifying resonance assignment.

Selective labeling is often achieved through exploitation of known metabolic pathways in organisms such as *Escherichia coli*. Such procedures have been primarily applied to protein systems (4,5); however, some selective labeling has also been done in nucleic acids (6,7), primarily for applications to dynamics. The high cost of selectively labeled late-stage intermediates has, nevertheless limited applicability. Labeling with random fractionally labeled early-stage substrates can be a more cost-effective alternative (8–10), but such randomly labeled metabolic substrates are not always available. Here we present a procedure for nucleotide labeling that relies on a combination of fully, but site-specifically, labeled early-stage substrates that may facilitate NMR structural application to RNAs and systems that use nucleotides as cofactors. Our own particular interest is in production of labeled guanosine diphosphate (GDP) for the study of GDP–GTP switch proteins. The anticipated structural data are from chemical shift anisotropy (CSA)-offsets and residual dipolar couplings. As an illustration we present some preliminary data on one such system.

^{13}C labeling of proteins using site-specifically labeled early-stage substrates has been documented previously in protein systems. For example, substitution of site-specifically labeled substrates, such as glucose (C1 and C2), glycerol (C1/C3 and C2) or pyruvate (C1 and C3), for uniformly labeled substrates leads to enhanced labeling at a subset of sites throughout expressed proteins (4,5,11–13). There can, of course, be some sacrifice in sensitivity by a reduction in percentage of labeling at certain sites, but as suggested above this is partially compensated by more efficient magnetization transfer and simpler spectra. Pulse sequences developed for magnetization transfer in uniformly enriched molecules typically require only minor modifications to take advantage of the spectral simplification seen in specifically labeled systems.

*To whom correspondence should be addressed. Tel: +1 706 542 6281; Fax: +1 706 542 4412; Email: jpresteg@ccrc.uga.edu

Nucleic acid structure determination has also benefited from isotopic labeling. Protocols to extract intact RNA from cells grown on uniformly isotopically labeled media and to isolate nucleoside monophosphates (NMPs) from the RNA have been described (6,14), but the use of specifically labeled precursors is less common (7,15). Isolating deoxyNMPs (dNMPs) is more difficult since cells contain 7–10 times more RNA than DNA (16), but this, too, has been described (17,18). Most protocols to extract NMPs from cell lysate call for the growth of *E.coli* in labeled minimal media to the late log phase for optimum ribosome production. Simple organic extractions easily separate proteins and lipids from the polymeric nucleic acids found in these structures (19).

Our initial motivation for the work described here included an attempt to take advantage of by-products from protein labeling efforts at the SECSG (20). Proteins expressed for the NMR core of the SECSG were grown in 98% ^{15}N ammonium chloride and a mixture of ^{13}C-1 and ^{13}C-2 glucose instead of uniformly labeled glucose; this yielded carbon enrichment at the 16–20% level in targeted proteins. The primary justification for this method was to initially reduce costs in large scale expression, but additional spectroscopic benefits have also been described (21). As discussed below, isolation of dNMPs and NMPs from cell debris proved difficult. In cells that have already been harvested and extracted of proteins, the lysate is frequently treated with deoxyribonuclease (DNAse I) to hydrolyze DNA and reduce the viscosity of the solution. In addition, most protein preparation protocols do not use RNAse-free techniques to preserve the ribosome and other readily isolatable sources of RNA. The mononucleoside phosphates (dNMPs and NMPs) that result from DNAse and RNAse hydrolysis are more difficult to isolate and extract than intact nucleic acids. Hence, *E.coli* was grown to late log phase with the isolation of labeled nucleotides specifically in mind.

The use of ^{13}C-1 and ^{13}C-2 glucose for partial labeling remains an important aspect in the studies described here. The low percentage ^{13}C enriched nucleotides isolated from *E.coli* grown with C-1 and C-2 labeled glucose should enjoy the same dilute spin advantages described for proteins. These nucleotides are particularly desirable over uniformly enriched nucleotides for measuring ^{13}C CSA-offsets and RDCs in aligned systems. The alignment of biomolecules in the magnetic field has produced a wealth of information on their structures and orientations. RDCs induced by low levels of order have been measured in a variety of molecules and alignment media (22–25). Chemical shift offsets can provide orientational constraints in a manner quite analogous to those provided by RDCs. They are particularly advantageous in providing constraints on nucleotide bases where all RDCs are in the plane of the base and the out-of-plane contributions of CSA-offsets are highly complementary. CSA-offsets have been measured for a number of biological systems where ordering is weak and long-range dipolar couplings cause minimal degradation of resolution (26–31). In the case of a more strongly aligned sample, (in membrane-associated systems, e.g. expected changes in chemical shift between isotropic and aligned resonances of aromatic carbons could reach tens of p.p.m. (32–35). However, under such strong alignment, multiple through-space dipolar couplings present in uniformly labeled samples produce coupled spectra with many poorly resolved splittings. Even ^{13}C–^{13}C one-bond scalar couplings in uniformly labeled samples contribute an additional 40 Hz, and two- and three-bond couplings produce an additional 7–11 Hz (36). When through-space dipolar couplings are present, the splittings are even more numerous. Hence, improved resolution is expected for partially labeled nucleotides, particularly if labels are nearly randomly distributed.

One example of the potential use of partially labeled nucleotides is to measure ^{13}C chemical shift offsets for nucleotide cofactors bound to membrane-associated GDP/GTP-binding GTPases or G proteins (37,38). RDCs have been used in combination with other NMR data to determine geometries of bound ligands in weakly aligned proteins (39–43), and it should be possible to use CSA-offset information in a similar way when systems are more strongly ordered. It is in these latter applications that partial labeling can be particularly advantageous.

RDCs from the protein itself have already been used to determine the molecular geometry of the membrane-associating GTPase ADP ribosylation factor 1 (ARF1) (44) and its orientation in weakly aligned systems (45). When more strongly aligned through association with a membrane, the CSA-offsets from ARF's isotopically labeled nucleotide-cofactor GDP or GTP may be more accessible and may prove a more useful probe of protein orientation relative to the membrane surface. To pursue such studies, it is important to have methods for producing partially labeled nucleotides and to know the details of labeling patterns for such molecules. Here we offer a fundamental analysis of isotopic labels in nucleotides extracted from *E.coli* grown on a mixture of C-1 and C-2 labeled glucose. We also present spectra demonstrating the enhanced signal to noise and improved resolution of partially ^{13}C-labeled GDP over uniformly labeled GDP when bound to ARF1, both in solution and in the presence of a model membrane. Although the extent of ordering in our particular system is less than in many membrane-anchored protein systems, it provides a stepping-stone to future studies of more strongly ordered systems with bound nucleotide cofactors as well as for large RNA systems.

MATERIALS AND METHODS

Cell growth and nucleoside monophosphate (NMP) isolation

All isotopes were purchased from Cambridge Isotope Laboratories, Inc. (Andover, MA). M9 media for growth of cells was prepared by adding per liter: 6 g $NaHPO_4$, 3 g KH_2PO_4, 0.5 g NaCl and 1 g NH_4Cl to ddH_2O and the solution was autoclaved. In addition, filter-sterilized solutions of the following were added to each liter: 15 ml 20% glucose, 1 ml 2.0 M $MgSO_4$, 1 ml metal mix (0.1 M $CaCl_2$, 0.1 M $MnCl_2$-$4H_2O$, 0.1 M $ZnSO_4$-$7H_2O$, 0.02 M $CoCl_2$-$6H_2O$, 0.02 M $CuCl_2$-$2H_2O$ and 0.02 M $NiCl_2$-$6H_2O$). A pET14 plasmid with no insert was transformed into *E.coli* BL21(DE3) Gold (Stratagene, La Jolla, CA) and plated onto M9 agar plates containing 100 μg/ml ampicillin. A single colony was used to inoculate 50 ml of M9 media containing 100 μg/ml ampicillin in a 250 ml baffled flask and grown overnight (~16 h) at 37°C while shaking at 250 r.p.m. One liter of M9 containing 100 μg/ml ampicillin, 1 g ^{15}N-NH_4Cl, 2 g 1-^{13}C-glucose and 1 g 2-^{13}C-glucose in a 2.5 l baffled flask was inoculated with

20 ml (1:50 dilution) of the overnight culture. The flask was grown at 37°C while shaking at 250 r.p.m. until OD_{600} = 0.7 (~3–4 h), moved to 22°C and the cells were harvested 16 h later. The cell pellets (~15 g) were immediately frozen at −70°C. Ribosomal RNA was extracted from thawed cells via French press, slow speed (SS-34) and high speed (Ti70) centrifugation and organic phase extraction according to Nikonowicz *et al*. (14). RNA was hydrolyzed to NMPs using P1 Nuclease (Roche), and the NMPs were eluted from a Vydac 3021.10C ion exchange high-performance liquid chromatography (HPLC) column (Grace Vydac, Hesperia, CA) with 50 mM ammonium formate, adjusted to pH 3.2 with formic acid (both from Aldrich, St Louis, MO). Peaks corresponding to CMP, UMP, AMP and GMP were collected separately, lyophilized, redissolved in water and lyophilized an additional two times to facilitate removal of volatile ammonium formate. Approximately 12 mg of each partially labeled NMP was recovered.

GDP synthesis

Since our target application is a GDP/GTP-binding switch protein (ARF1), GMP was converted to GDP, and for comparison purposes, this was done with both partially labeled and fully labeled starting materials. Fully labeled GDP was synthesized from >98% ^{13}C, ^{15}N GMP (Spectra Stable Isotopes, Columbia, MD), and partially labeled GDP was synthesized from the GMP described above, both using a modified protocol from Niconowicz *et al*. (14). Guanylate Kinase (Sigma) was used to phosphorylate GMP and excess ATP (Sigma) was added as the phosphate donor. The reaction was maintained at 37°C for 44–48 h and then quenched by addition of 100 µl of 50 mM EDTA. The volume was reduced to half by lyophilization, and absolute ethanol was added to three times the volume with overnight storage at −20°C to effect precipitation of nucleotides. The precipitated nucleotides were dried in air, dissolved in water and purified by HPLC using the Vydac 3021.10C ion exchange column and a 35 ml step gradient of 50, 100 and 200 mM ammonium formate (pH 3.2). Fractions were lyophilized, redissolved in water and lyophilized again to facilitate removal of formate. The yield from this separation was 50–65%.

Nucleotide exchange

^{15}N-labeled ARF1 was prepared according to methods described previously (44). ^{13}C and ^{15}N GDP was exchanged into ARF1 by an EDTA-mediated exchange. A 25-fold excess of EDTA over ARF1 was added to a solution of 0.5 mM ARF1 to remove magnesium and facilitate turnover of native nucleotide. This was followed by addition of a 10-fold excess of ^{13}C and ^{15}N GDP in buffer containing 20 mM Tris–HCl (pH 7.6), 100 mM NaCl, 5 mM $MgCl_2$ and 2 mM NaN_3. The exchange took place for 48 h at 4°C. EDTA was removed from the solution by several serial dilutions with the above buffer minus GDP until the final estimated concentration of EDTA was <30 nM.

Alignment medium preparation

$C_{12}E_5$/hexanol has previously been identified as a suitable alignment medium for both ARF1 (45) and a lipid that interacts with ARF1 at a membrane surface, PIP_2 (46). This medium was prepared as follows: Pentaethylene glycol monododecyl ether $C_{12}E_5$ (Sigma, St Louis, MO) was combined with hexanol in the ratio 0.88:1 to make a solution of 4.6% (w/w) $C_{12}E_5$ (47–49). Pure PIP_2 [phosphatidylinositol 4,5-bisphosphate, Avanti Polar Lipids, (Alabaster, AL)], was dried under a stream of nitrogen and added directly to the $C_{12}E_5$ bilayers at a relatively low molar ratio of PIP_2 to $C_{12}E_5$ (1:80) so that bilayer order is not disrupted. ARF1 was added to the medium to produce a final solution of ~0.7–1.0 mM protein at a 2:1 PIP_2 to ARF1 ratio.

NMP NMR analysis

NMP fractions were analyzed by ^{1}H, ^{13}C and ^{31}P NMR on a 500 MHz Varian (Palo Alto, CA) Inova spectrometer using a triple resonance Varian probe for ^{1}H, a 5 mm Nalorac $^{13}C/^{15}N$ broadband observe probe (operating at 125.6 MHz) for ^{13}C, and a 5 mm Varian broadband observe probe (operating at 202.6 MHz) for ^{31}P spectra. ^{13}C spectra were collected with a 45° tip angle, rapid recycling (0.5 s recycle delay), and Waltz-16 ^{1}H decoupling for NOE enhancement. All spectra were collected at 25° C. These spectra were used to determine chemical shifts (and ^{13}C–^{1}H scalar couplings by turning off the proton decoupling during acquisition). Relative peak intensities were determined by integrating peaks observed with decoupling during acquisition only and a long recycle delay (5 s) to allow sufficient magnetization recovery. ^{31}P observe and 1D ^{1}H–^{31}P HMQC spectra were collected to confirm ribose phosphorylation (data not shown). The pH of each sample was recorded, and free phosphate was added to 0.85–1.65 mM to each HPLC fraction as a reference signal for determination of ^{31}P chemical shift and nucleotide concentration. ^{13}C chemical shifts were referenced indirectly by referring to added DSS and using appropriate ratios for properly referenced ^{13}C spectra (50,51).

GDP-Bound ARF1 NMR analysis

^{13}C direct observe data on an ARF1 complex containing labeled GDP were collected at 25°C on an 800 MHz Varian Inova spectrometer using the normal ^{13}C decoupling input on a triple resonance Varian Chili Probe in a 4 mM D_2O susceptibility-matched Shigemi (Alison Park, PA) tube. ^{13}C spectra were collected with a 33–45° tip angle and Waltz-16 ^{1}H decoupling at a B_1 field of 12 000 Hz during acquisition. For 98% ^{13}C-GDP isotropic samples, 30 000–40 000 scans were acquired, and for aligned samples 83 000 scans were acquired, both with a 1.6 s recycle time. For 13% ^{13}C-GDP isotropic samples, 300 000 scans were acquired, and for aligned samples 630 000 scans were acquired, both with rapid recycling (0.3 s recycle time). ^{15}N–^{1}H heteronuclear single quantum coherence spectra (HSQC) were also collected before and after each ^{13}C experiment (data not shown) to confirm protein integrity. Liquid crystal alignment was also confirmed by monitoring the ^{2}H NMR quadrupolar splitting of water deuterons (18–21 Hz). Protein alignment was independently determined by measuring ^{15}N–^{1}H RDCs on the lipid-doped $C_{12}E_5$ model membrane sample (data not shown). ^{13}C spectra were processed using NMRPipe (52), applying backwards linear prediction and an exponential apodization function with a 30 Hz line broadening constant. The automated lineshape fitting routine within NMRPipe (nlinLS) was used in

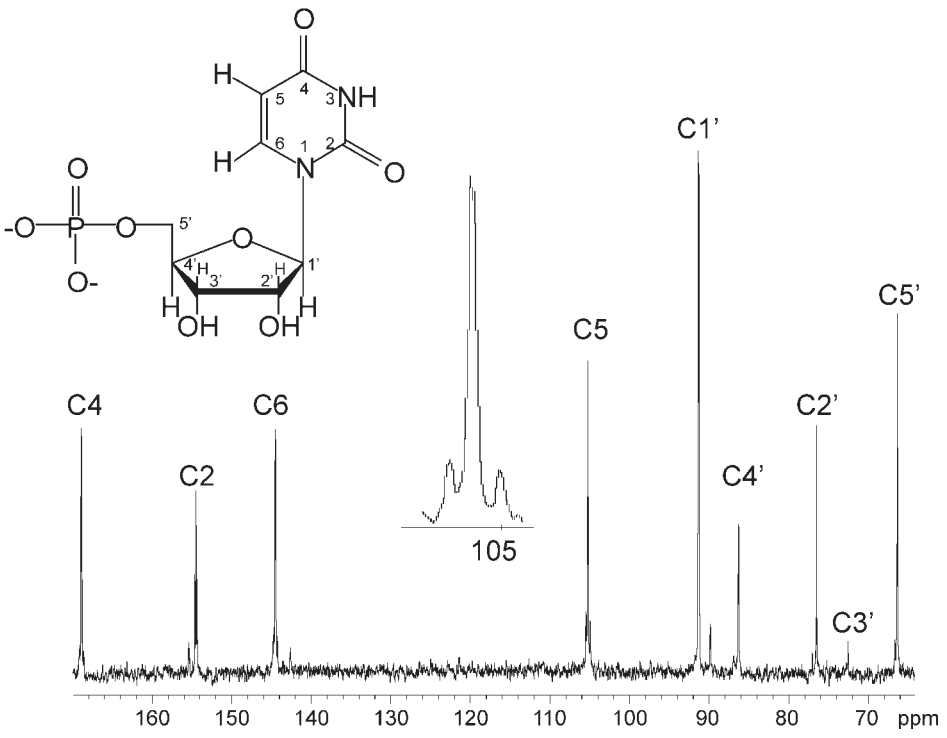

Figure 1. ^{13}C NMR spectrum of base and ribose regions of UMP. Small tip angles (45°) and long recycle delay times (5.0 s) were used to promote uniform carbon relaxation. Assignments were based on published spectra (36). Inset shows low intensity ^{13}C satellites for C5.

order to accurately extract resonance positions. ^{13}C and ^{15}N chemical shifts in the protein samples were referenced indirectly by referencing to added DSS and using appropriate ratios for properly referenced ^{13}C or ^{15}N spectra, respectively.

RESULTS

In Figure 1 the ^{13}C NMR spectrum of both the base and ribose regions for UMP is shown as a representative of other nucleotide spectra. Chemical shift assignments are based on previously reported data (36). Note, that the C1′ carbon shows the highest level of carbon labeling. Peak intensities vary due to the differing levels of enrichment, as dictated by their origin in biosynthetic pathways. Most other ribose and base carbons show moderate levels of labeling as evidenced by ^{13}C spectra; the lack of ^{13}C–^{13}C couplings (except at the bases of peaks, e.g. to C5 shown in Figure 1 inset) also shows low probabilities of simultaneous labeling at adjacent sites.

In Figure 2 expansions of the base region in ^{13}C NMR spectra of each of the NMPs are shown. C5 and C6 of pyrimidines (Figure 2a for CMP, Figure 2b for UMP) appear to get labeled at approximately the same percentage, and C2 and C4 show significantly lower intensities. These differing intensities are due, in part, to the nuclear overhauser enhancement (NOE) for protonated carbons, C5 and C6. A small amount of AMP was present in the UMP spectrum, as noted by asterisks. In purine (Figure 2c for AMP, Figure 2d for GMP) spectra, we observed ^{13}C labeling of C2, C5, C6 and C8 and almost no ^{13}C labeling of C4 (Figure 2c and d). C2 and C8 show similar labeling levels in both AMP and GMP. C5 and C6 exhibit lower, but approximately equal levels of isotopic labels. The AMP fraction was contaminated with about 10% UMP, represented in Figure 2c by asterisks. Several one-bond ^{13}C–^{15}N scalar couplings are observed in ^{13}C spectra, e.g. the barely observable splittings seen at the top of the peaks for C4 and C6 of UMP and CMP (Figure 2a and b).

In Table 1 we summarize the chemical shifts for the four NMPs as well as estimates of isotopic enrichment. We estimate the level of carbon enrichment based on ^{13}C resonance intensities collected with long recycle delays (data not shown) and on ^{13}C satellites in ^{1}H spectra (Figure 3). The H6 proton signal from CMP (Figure 3a), e.g. shows ^{13}C satellites that represent 29% of the total incorporation. H1′ is the only ribose sugar proton resonance with appreciable ^{13}C satellites. Satellites for H5 and H1′ resonances (Figure 3b) of CMP show about 31% ^{13}C incorporation for H5 and 45% for H1′.

In Figure 4a and b we present ^{13}C spectra from the aromatic region of 13% ^{13}C-labeled GDP-bound to ARF1 when aligned (Figure 4a) and in isotropic buffer solution (Figure 4b), respectively. The aligned sample is oriented in a 4.6% (w/w) $C_{12}E_5$ bilayered liquid crystal doped with PIP_2, a signaling lipid that is suggested to interact with ARF1 (53–55). Aromatic base carbon frequencies are labeled for easily observed resonances; C4 and C6 are not observed due to lower levels of isotopic incorporation. Unlabeled regions of high spectral intensity represent natural abundance ^{13}C protein signals from aromatic (~130 p.p.m.) resonances; these are marked with double asterisks. Some free GDP (denoted by a single asterisk) is also observed in isotropic solution, and resonances from this free GDP are readily identified based on distinct chemical shifts between free and bound forms. Chemical shift offsets between isotropic and aligned spectra, though small, are

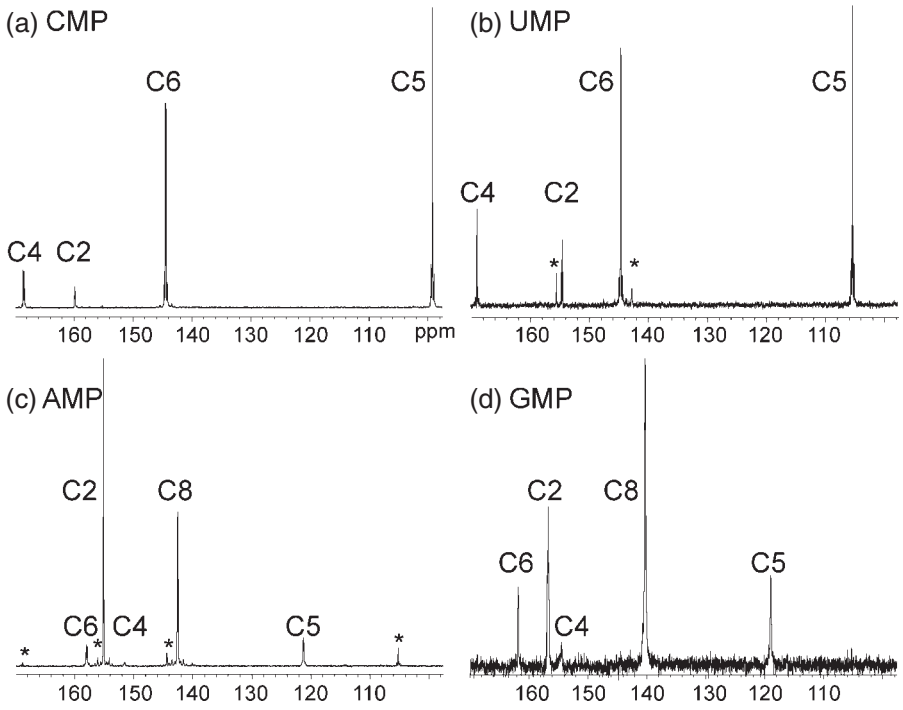

Figure 2. ^{13}C (^{1}H-decoupled) NMR spectra of the base region of NMPs using 5.0 s recycle rates: (**a**) CMP, (**b**) UMP, (**c**) AMP and (**d**) GMP. Assignments were based on published spectra (36). Asterisks represent contaminating peaks from other nucleotides.

Table 1. ^{13}C chemical shifts (p.p.m.) of labeled NMPs and site-specific percentage of isotopic incorporation

^{13}C	CMP			UMP			AMP			GMP		
	Chemical shift (p.p.m.)	Relative %label[a]	Absolute %label[b]	Chemical shift (p.p.m.)	Relative %label[a]	Absolute %label[b]	Chemical shift (p.p.m.)	Relative %label[a]	Absolute %label[b]	Chemical shift (p.p.m.)	Relative %label[a]	Absolute %label[b]
C2	159.8	32	14	154.5	39	16	155.1	73	38	156.8	66	22
C4	168.5	46	21	168.9	41	16	151.5	7	4	154	–	<2
C5	99.3	68	31	105.2	72	29	121.2	40	21	118.9	37	12
C6	144.5	64	29	144.5	61	24	157.9	31	16	161.8	28	9
C8	–	–	–	–	–	–	142.6	70	36	140.3	57	19
C1′	92.1	100	45	91.3	100	40	89.9	100	52	89.6	100	33
C2′	77.0	26	12	76.5	30	12	77.0	26	14	76.6	26	9
C3′	72.3	8	4	72.4	11	4	73.1	5	3	73.2	7	2
C4′	85.8	29	13	86.3	35	14	86.7	24	12	86.7	35	12
C5′	66.3	63	28	66.4	58	23	66.8	52	27	67.2	42	14

[a]Percentage labeling determined relative to C1′ peak intensity by integrating ^{13}C peak intensities in fully relaxed ^{13}C spectra.
[b]Percentage determined by integrating ^{13}C satellites to H1′ in ^{1}H spectra and using relative ^{13}C percentage labels.

observed for the aromatic carbons, with C2 and C5 displaying differential shifts with C2 moving downfield (54 Hz). These differences are likely to arise from orientational dependences of CSAs, and they can be structurally useful.

The resolution and quality of some signals, e.g. C2, is also significantly better than what can be obtained under comparable conditions with a 98% carbon-labeled sample. Figure 5a and b show expansions of the C2 region of the spectrum for similarly aligned samples using a 13% carbon-labeled sample (Figure 5a) and a 98% carbon-labeled sample (Figure 5b). The resonance is considerably broader for the 98% sample and the signal to noise ratio appears less despite the fact that the additional scans for the 13% sample (a factor of 8) are not nearly enough to compensate for the decrease in ^{13}C content by a factor of 7.5. Even if repetition times were the same in both acquisitions (it was shorter for the 13% sample), this factor would need to be squared to fully compensate for decreased label content.

DISCUSSION

Improved resolution in spectra of partially labeled NMPs

There is little doubt that reduction of percent labeling, when done approximately randomly, results in an improvement in signal quality despite somewhat lower overall sensitivity. We suggest that the absence of significant ^{13}C–^{13}C splittings from both scalar and long-range dipolar couplings is the origin of this improvement. One would expect broadening of resonances and loss of signal due to unresolved splittings of resonances when enrichment is high or if labeled pairs were

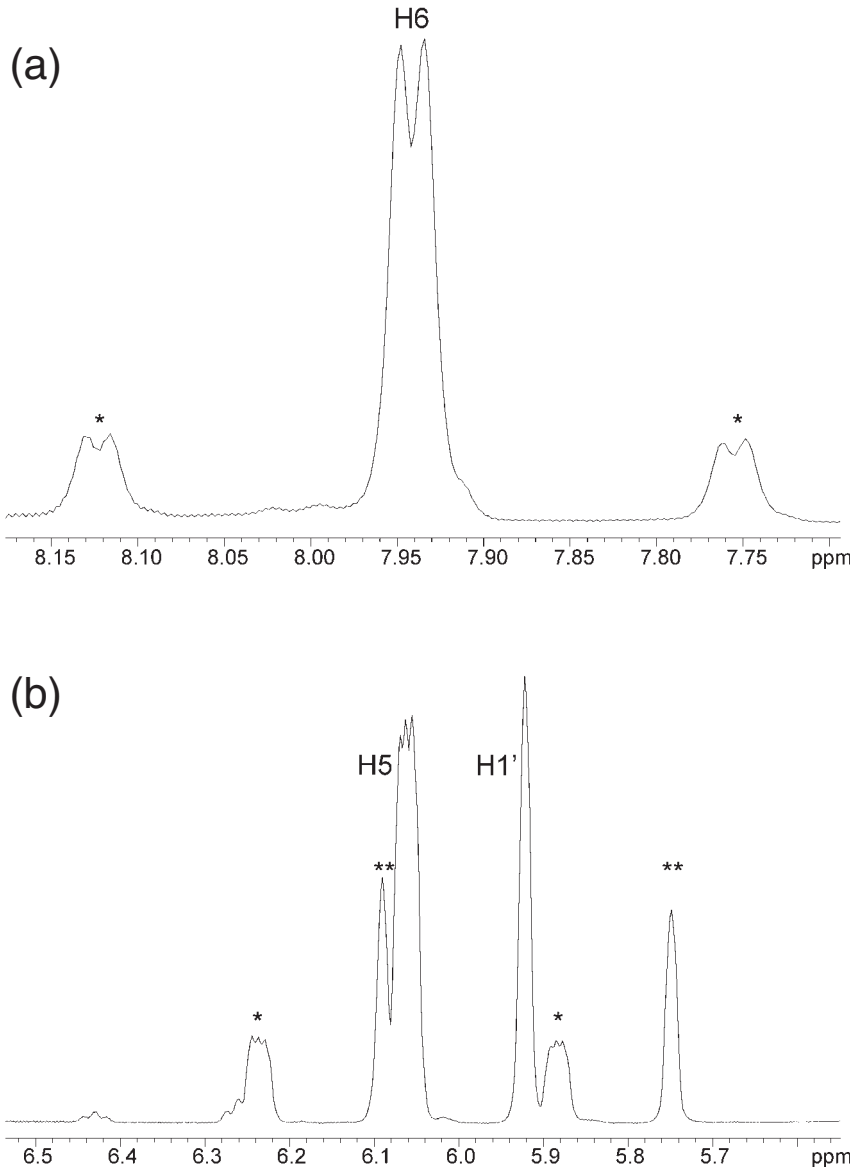

Figure 3. ^{1}H NMR of CMP's (**a**) aromatic region (H6) and (**b**) anomeric region (H5 and H1′). ^{13}C satellites are observed for all three ^{1}H peaks and are represented by a single asterisk for H5 and H6 and a double asterisk for H1′. Assignments were based on published spectra (36).

incorporated as intact units. We do not see scalar couplings at 13% enrichment under high resolution, non-protein-bound, conditions (Figures 1 and 2) and we would expect fewer dipolar couplings under aligned conditions as well. Resonance intensity, even if reduced by partial labeling, would be largely concentrated into a single resonance resulting in an improvement in resonance quality.

Biosynthetic pathways lead to desirable labeling: Pentose Phosphate Pathway (PPP) yields labeled ribose

Near random labeling, or labeling only of selected sites, is essential to the gains from the absence of scalar or dipolar coupling described above. The labeling patterns observed for the systems studied here can be understood based on well-known biosynthetic pathways for ribose and the nucleotide bases. The use of ^{13}C NMR has long been important in the elucidation of metabolic pathways (56–58) as well as in the introduction of ^{13}C isotopic labels into proteins of interest. Less discussion exists for isotopic labeling of nucleotides, and none exists specifically for the use of C-1 and C-2 glucose mixture in *E.coli* growth. Here we attempt to rationalize the isotopic labeling pattern of nucleic acids grown with ^{13}C labeling from C-1 and C-2 glucose.

Unlike most amino acids of proteins, where ^{13}C labels from C-1 and C-2 glucose mixtures are nearly uniformly distributed across alpha, carbonyl and other carbons, ribose carbons are highly enriched at the C-1 position. Ribose-5-phosphate (R5P), the precursor to ribose in all nucleotides is produced directly from glucose and glucose-6-phosphate (G6P) in the PPP by the elimination of C-1 from glucose (Figure 6). Depending on the cell's metabolic needs, 6GP can either undergo isomerization to fructose 6-phosphate (F6P) by phosphoglucose isomerase or oxidation and hydrolysis to 6-phosphogluconate (6PG) by

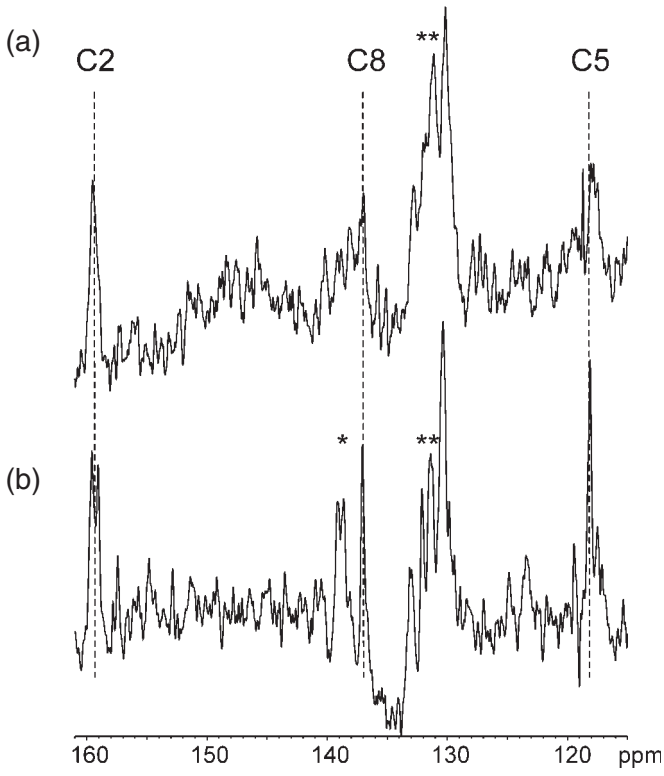

Figure 4. ^{13}C (^{1}H-decoupled) NMR spectra of the aromatic region of GDP-bound ARF1: (**a**) 13% ^{13}C-GDP-ARF1 (1.0 mM) in aligned $C_{12}E_5$-PIP_2 model-membranes (630 000 scans, 0.3 s recycle time) and (**b**) 13% ^{13}C-GDP-ARF1 (1.4 mM) in isotropic buffer solution (300 000 scans, 0.3 s recycle time). A single asterisk represents free GDP in solution, and a double asterisk represents unlabeled aromatic carbons from ARF1. Vertical lines indicate observed shift offsets between isotropic and aligned carbons.

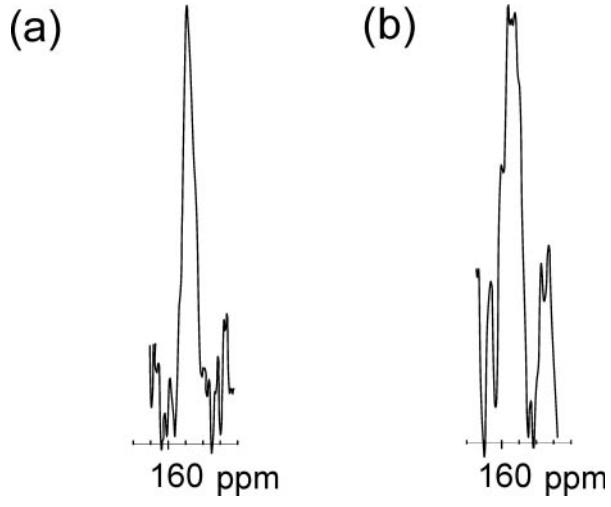

Figure 5. Expansion of ^{13}C (^{1}H-decoupled) NMR spectral regions for the C2 carbon of GDP in GDP-bound ARF1 when aligned in 4.6% $C_{12}E_5$-PIP_2 model-membranes using (**a**) 13% ^{13}C-GDP (630 000 scans, 0.3 s recycle time) and (**b**) 98% ^{13}C-GDP (83 000 scans, 1.6 s recycle time). Resolution is improved for 13% ^{13}C-GDP-ARF1 compared to 98% ^{13}C-GDP-ARF1.

6GP dehydrogenase and 6-phosphoglucono lactonase, respectively. The subsequent oxidative decarboxylation of 6PG by phosphogluconate dehydrogenase to ribulose-5-phosphate (Ru5P) is the final step in the oxidative portion of the pentose

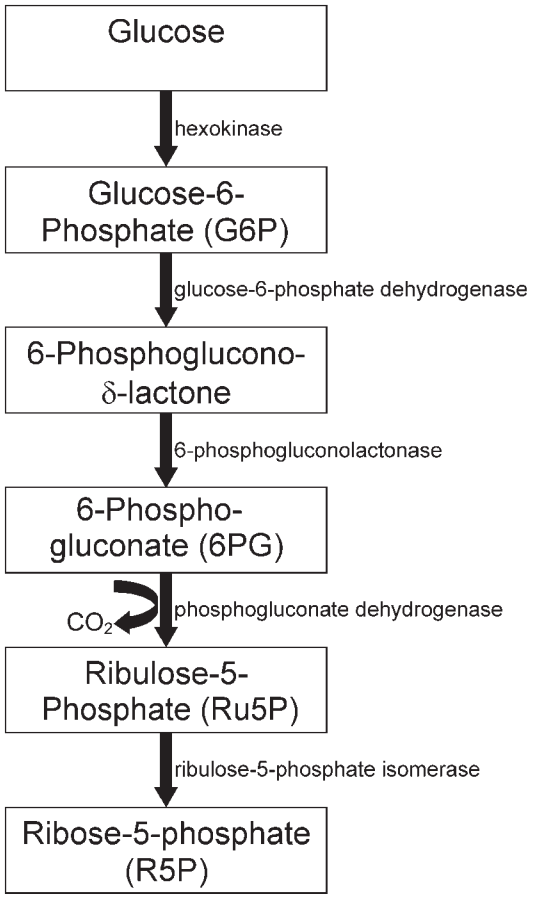

Figure 6. The PPP and the predominant pathway for R5P synthesis (61).

phosphate pathway. Isomerization of Ru5P to ribose-5-phosphate (R5P) by Ru5P isomerase is controlled by the cell's metabolic needs. R5P is then utilized in nucleotide biosynthesis (59). Hence, the enriched carbon of the C-2 glucose used in our minimal media for *E.coli* growth has a direct route to the C1 of ribose, and nucleotides thus become highly enriched at C1′, as shown in Table 1.

Some labeling of ribose carbons C2′, C4′ and C5′ is also observed (Figure 2), but C3′ shows almost no ^{13}C enrichment (Table 1). The labeling pattern can be rationalized as follows. The recycling of cellular components with near random levels of isotopic incorporation results in low labeling levels for most ribose carbons. Specifically, glycolysis and gluconeogenesis scramble the C-1 and C-2 labels such that C1′, C2′, C5′ and C6′ of glucose all become labeled. In addition, the PPP regenerates glucose with C1′ and C3′ labels (60–62). However, C4′ does not become labeled through any of the above pathways. The final labeling scheme results in isotopic labels everywhere except C4′ of glucose. Due to the decarboxylation discussed above, C4′ of glucose becomes C3′ of ribose, and little labeling of ribose C3′ is observed.

Purine base biosynthesis

Labeling patterns in nucleotide base biosynthesis can be understood by considering isotopic labeling of their precursors. In the case of purines, labeling can be rationalized by

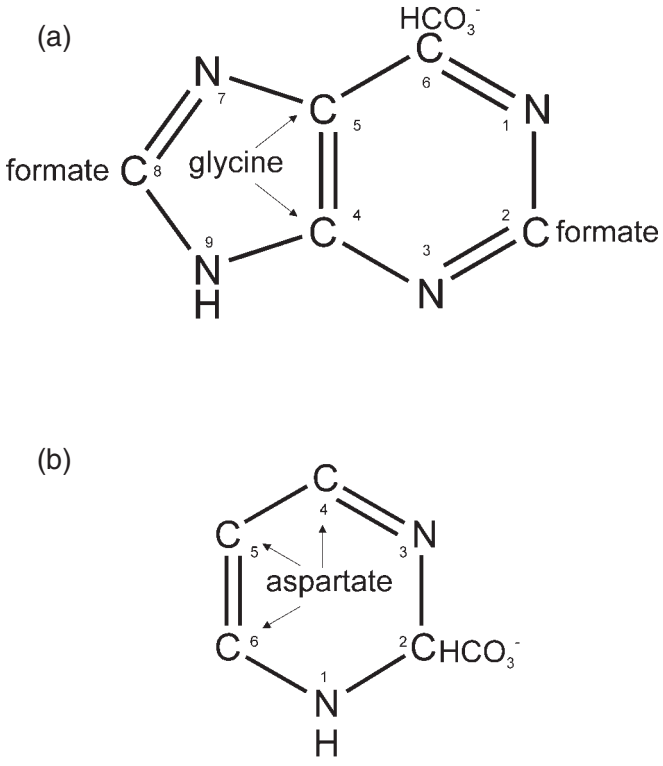

Figure 7. Predicted biosynthetic carbon sources for (**a**) purines and (**b**) pyrimidines (59).

considering the origin from constitutive amino acids, formate and bicarbonate (Figure 7a). C2 and C8 are derived from a formyl group transferred by N10-formyl-tetrahydrofurate. C6 is derived from bicarbonate. These one carbon sources are labeled by metabolic degradation of glucose. The single carbon pool is diluted by ^{12}C carbons, hence labeling of these groups is at a lower level and essentially random. C4 and C5 are derived from the C′ and Cα carbons, respectively, from glycine. Glycine, synthesized in the linear part of amino acid biosynthesis from serine, should incorporate an isotopic label at Cα, but the carbonyl carbon is not predicted to be labeled in *E.coli* grown on C-1 glucose or C-2 glycerol (12). In our purine (AMP and GMP) spectra, we observed significant ^{13}C labeling of C2, C5, C6 and C8, and almost no ^{13}C labeling of C4 (Figure 3c and d). As C4 comes from the carbonyl carbon of glycine, the lack of labeling in our system is consistent with previous predictions for amino acids in similar growth media (12).

Pyrimidine base biosynthesis

Pyrimidines differ from purines in that they are almost entirely synthesized from aspartate (Figure 7b). Biochemical pathways indicate aspartic acid carbons form pyrimidines as follows: Cα forms C6, Cβ forms C5, Cγ forms C4. The C2 originates from bicarbonate. Theoretical and experimental analysis of a selectively, but extensively, labeled protein indicates all aspartate carbons should eventually become labeled with ^{13}C-1 and ^{13}C-2 glucose through the citric acid cycle, but at lower levels for Cγ and C′ (12,13,63). Aspartic acid is generated from oxaloacetate, which in turn can arise from direct carboxylation of pyruvate or from the citric acid cycle. Aspartate formed from pyruvate carboxylation lacks both the Cγ and C′ label; whereas, aspartate synthesized from oxaloacetate derived from the citric acid cycle has highly enriched labels at Cα and Cβ and lower levels of labeling at Cγ and C′. C5 and C6 of CMP and UMP appear to get labeled at approximately the same percentage, consistent with Cα and Cβ of aspartic acid being labeled. The lower level of enrichment for C4 is consistent with the predicted low level of labeling at Cγ in similar media (12). In all cases the precursors start with glucose molecules containing a single ^{13}C, and these single sites are diluted with ^{12}C in metabolic intermediates. Hence, there is little possibility of having directly bonded ^{13}C's.

Isolation of NMPs as by-products from protein expression

While we found it advantageous to grow cells explicitly for the purpose of isolating RNA and subsequently NMPs, the prospect of recovering these as by-products of protein synthesis remains appealing. A one liter growth of cells for protein expression requiring 3 g ^{13}C glucose and 1 g ^{15}N ammonium chloride typically leaves a significant amount of isotopically labeled biological waste. Given that a typical *E.coli* cell is composed of about 55% protein, 20% RNA, 9% lipid and 3% DNA by weight (16), this represents a significant source of RNA and NMPs. The reasons for our lack of success in isolation are not entirely clear. However, cells grown to the mid-log phase for isopropyl-β-D-thiogalactopyranoside (IPTG) induction and protein overexpression either may produce much less RNA than cells grown to the late log phase, as is typically done for RNA preps, or RNA in these preps may be degraded during protein isolation, yielding mononucleotides that are difficult to recover. In either case, minor modifications of protein production protocols may facilitate recovery of NMPs.

Use of partially labeled NMPs in structural NMR studies

It is clear from our work on the ARF1 protein system that partially labeled nucleotide samples can give useable spectra in complex biochemical systems. This work opens opportunities for monitoring nucleotide cofactor behavior in many protein systems, as well as RNA behavior when produced by conversion of NMPs to nucleotide triphosphates. One way to exploit spectra from these materials is to capitalize on offsets in resonance position that come from chemical shift anisotropies when samples are partially oriented. Chemical shift anisotropies for carbons in the rings of nucleotide bases are large (i.e. 108 p.p.m. for C2 and 114 p.p.m. for C8 of guanine) (64) e.g. with the most shielded component perpendicular to the base ring. If the protein were to orient with the GDP ring plane preferentially perpendicular to the magnetic field, the C2 and C8 resonances would move downfield relative to resonances with lower chemical shift anisotropies such as C5 and the ribose C1′ carbon. While shift offsets in our system, which is not strongly associated with the membrane-like bicelles of the alignment medium (ordering just a few parts in 10 000), are small, offsets calculated with order parameters on the order of 10^{-3} give large enough shift offsets (one-tenth of a p.p.m.) to measure accurately and interpret quantitatively. The myristoylated form of GDP-bound ARF1, e.g. would be expected to orient more strongly (perhaps

10^{-2}) through myristoyl chain—$C_{12}E_5$ bilayer interactions and display much larger shift offsets. This would give a picture of membrane–protein interaction geometry through the nucleotide-cofactor reporter. We expect the partially labeled material and the approach to its production described here to be useful in such studies.

CONCLUSIONS

We have presented the ^{13}C isotopic labeling patterns of NMPs extracted from *E.coli* grown on a less commonly used mixture of C-1 and C-2 glucose. By comparing our results to previously observed data on amino acids grown in similar media and relying on the well-known biochemistry of nucleotide biosynthesis, we have been able to rationalize the labeling pattern. Despite a few notable absences (C4 in purines and C3′ in ribose) and one more highly labeled site (C1′ in ribose), most carbons are randomly labeled at a low level. With the low level of labeling, scalar couplings and additional splitting from long-range dipolar couplings are minimized, affording greater spectral quality than seen in fully labeled materials. This should allow high resolution measurement of structurally useful parameters such as chemical shift anisotropy-offsets in weakly aligned liquid crystals. Application to studies of proteins with nucleotide cofactors, particularly in their membrane-associated states where direct observation of ^{13}C is preferred to observation of more strongly relaxing proton signals, should soon be possible.

ACKNOWLEDGEMENTS

The authors thank Dr Kristen Mayer, Prof. Pascale Legault and Prof. John Marino for helpful discussions and Shan Liu for NMP isolation assistance. The authors also thank Dr Ron Seidel and Brett Israel for providing protein. This work is supported by a grant from the National Institutes of Health (GM61268). Funding to pay the Open Access publication charges for this article was provided by a grant from the NIH (GM61268).

Conflict of interest statement. None declared.

REFERENCES

1. Clore,G.M. and Gronenborn,A.M. (1994) Multidimensional heteronuclear nuclear magnetic resonance of proteins. *Methods Enzymol*., **239**, 349–363.
2. Bax,A. (1994) Multidimensional nuclear magnetic resonance methods for protein studies. *Curr. Opin. Struct. Biol*., **4**, 738–744.
3. Mollova,E.T. and Pardi,A. (2000) NMR solution structure determination of RNAs. *Curr. Opin. Struct. Biol*., **10**, 298–302.
4. LeMaster,D.M. and Kushlan,D.M. (1996) Dynamical mapping of *E.coli* thioredoxin via ^{13}C NMR relaxation analysis. *J. Am. Chem. Soc*., **118**, 9255–9264.
5. Lian,L.Y. and Middleton,D.A. (2001) Labelling approaches for protein structural studies by solution-state and solid-state NMR. *Proc. Nucl. Magn. Reson. Spectrosc*., **39**, 171–190.
6. Batey,R.T., Battiste,J.L. and Williamson,J.R. (1995) Preparation of isotopically enriched RNAs for heteronuclear NMR. *Nucl. Magn. Reson. Nucleic Acids*, **261**, 300–322.
7. Scott,L.G., Tolbert,T.J. and Williamson,J.R. (2000) Preparation of specifically ^{2}H- and ^{13}C-labeled ribonucleotides. *Methods Enzymol*., **317**, 18–38.
8. Wand,A.J., Bieber,R.J., Urbauer,J.L., McEvoy,R.P. and Gan,Z.H. (1995) Carbon relaxation in randomly fractionally ^{13}C-enriched proteins. *J. Magn. Reson. B*, **108**, 173–175.
9. Boisbouvier,J., Brutscher,B., Simorre,J.P. and Marion,D. (1999) ^{13}C spin relaxation measurements in RNA: sensitivity and resolution improvement using spin-state selective correlation experiments. *J. Biomol. NMR*, **14**, 241–252.
10. Kojima,C., Ono,A., Kainosho,M. and James,T.L. (1998) DNA duplex dynamics: NMR relaxation studies of a decamer with uniformly ^{13}C-labeled purine nucleotides. *J. Magn. Reson*., **135**, 310–333.
11. Gardner,K.H. and Kay,L.E. (1998) The use of ^{2}H, ^{13}C, ^{15}N multidimensional NMR to study the structure and dynamics of proteins. *Annu. Rev. Biophys. Biomol. Struct*., **27**, 357–406.
12. Hong,M. (1999) Determination of multiple phi-torsion angles in proteins by selective and extensive ^{13}C labeling and two-dimensional solid-state NMR. *J. Magn. Reson*., **139**, 389–401.
13. Castellani,F., van Rossum,B., Diehl,A., Schubert,M., Rehbein,K. and Oschkinat,H. (2002) Structure of a protein determined by solid-state magic-angle-spinning NMR spectroscopy. *Nature*, **420**, 98–102.
14. Nikonowicz,E.P., Sirr,A., Legault,P., Jucker,F.M., Baer,L.M. and Pardi,A. (1992) Preparation of ^{13}C and ^{15}N labeled RNAs for heteronuclear multidimensional NMR-studies. *Nucleic Acids Res*., **20**, 4507–4513.
15. Tolbert,T.J. and Williamson,J.R. (1997) Preparation of specifically deuterated and ^{13}C-labeled RNA for NMR studies using enzymatic synthesis. *J. Am. Chem. Soc*., **119**, 12100–12108.
16. Neidhardt,F.C. and Umbarger,H.E. (1996) Chemical composition of *Escherichia coli*.. In Neidhardt,F.C. (ed.), *Escherichia coli and Salmonella: Cellular and Molecular Biology, 2nd edn.* ASM Press, Washington, DC, Vol. 1, pp. 13–16.
17. Zimmer,D.P. and Crothers,D.M. (1995) NMR of enzymatically synthesized uniformly ^{13}C–^{15}N-labeled DNA oligonucleotides. *Proc. Natl Acad. Sci. USA*, **92**, 3091–3095.
18. Smith,D.E., Su,J.Y. and Jucker,F.M. (1997) Efficient enzymatic synthesis of ^{13}C, ^{15}N-labeled DNA for NMR studies. *J. Biomol. NMR*, **10**, 245–253.
19. Sambrook,J., Fritsch,E.F. and Maniatis,T. (1989) *Molecular Cloning: A Laboratory Manual, 2nd edn*. Cold Spring Harbor Laboratory, Cold Spring Harbor, NY.
20. Adams,M.W.W., Dailey,H.A., Delucas,L.J., Luo,M., Prestegard,J.H., Rose,J.P. and Wang,B.C. (2003) The southeast collaboratory for structural genomics: a high-throughput gene to structure factory. *Acc. Chem. Res*., **36**, 191–198.
21. Tian,F., Valafar,H. and Prestegard,J.H. (2001) A dipolar coupling based strategy for simultaneous assignment and structure determination of protein backbones. *J. Am. Chem. Soc*., **123**, 11791–11796.
22. Hansen,M.R., Hanson,P. and Pardi,A. (2000) Filamentous bacteriophage for aligning RNA, DNA, and proteins for measurement of nuclear magnetic resonance dipolar coupling interactions. *Methods Enzymol*., **317**, 220–240.
23. Bax,A. (2003) Weak alignment offers new NMR opportunities to study protein structure and dynamics. *Protein Sci*., **12**, 1–16.
24. Prestegard,J.H. and Kishore,A.I. (2001) Partial alignment of biomolecules: an aid to NMR characterization. *Curr. Opin. Chem. Biol*., **5**, 584–590.
25. Prestegard,J.H., Bougault,C.M. and Kishore,A.I. (2004) Residual dipolar couplings in structure determination of biomolecules. *Chem. Rev*., **104**, 3519–3540.
26. Sanders,C.R. (1993) Solid-state ^{13}C NMR of unlabeled phosphatidylcholine bilayers: spectral assignments and measurement of carbon–phosphorus dipolar couplings and ^{13}C chemical shift anisotropies. *Biophys. J*., **64**, 171–181.
27. Lipsitz,R.S. and Tjandra,N. (2001) Carbonyl CSA restraints from solution NMR for protein structure refinement. *J. Am. Chem. Soc*., **123**, 11065–11066.
28. Lipsitz,R.S. and Tjandra,N. (2003) ^{15}N chemical shift anisotropy in protein structure refinement and comparison with NH residual dipolar couplings. *J. Magn. Reson*., **164**, 171–176.
29. Choy,W.Y., Tollinger,M., Mueller,G.A. and Kay,L.E. (2001) Direct structure refinement of high molecular weight proteins against residual dipolar couplings and carbonyl chemical shift changes upon alignment: an application to maltose binding protein. *J. Biomol. NMR*, **21**, 31–40.

30. Wu,Z.R., Tjandra,N. and Bax,A. (2001) ^{31}P chemical shift anisotropy as an aid in determining nucleic acid structure in liquid crystals. *J. Am. Chem. Soc.*, **123**, 3617–3618.
31. Boyd,J. and Redfield,C. (1999) Characterization of ^{15}N chemical shift anisotropy from orientation-dependent changes to ^{15}N chemical shifts in dilute bicelle solutions. *J. Am. Chem. Soc.*, **121**, 7441–7442.
32. Losonczi,J.A. and Prestegard,J.H. (1998) NMR characterization of the myristoylated, N-terminal fragment of ADP-ribosylation factor 1 in a magnetically oriented membrane array. *Biochemistry*, **37**, 706–716.
33. Gu,Z.T.T. and Opella,S.J. (1999) Two- and three-dimensional ^{1}H/^{13}C PISEMA experiments and their application to backbone and side chain sites of amino acids and peptides. *J. Magn. Reson.*, **140**, 340–346.
34. Valentine,K.G., Mesleh,M.F., Opella,S.J., Ikura,M. and Ames,J.B. (2003) Structure, topology, and dynamics of myristoylated recoverin bound to phospholipid bilayers. *Biochemistry*, **42**, 6333–6340.
35. Wang,J., Denny,J., Tian,C., Kim,S., Mo,Y., Kovacs,F., Song,Z., Nishimura,K., Gan,Z., Fu,R. *et al.* (2000) Imaging membrane protein helical wheels. *J. Magn. Reson.*, **114**, 162–167.
36. Ippel,J.H., Wijmenga,S.S., deJong,R., Heus,H.A., Hilbers,C.W., deVroom,E., vanderMarel,G.A. and vanBoom,J.H. (1996) Heteronuclear scalar couplings in the bases and sugar rings of nucleic acids: their determination and application in assignment and conformational analysis. *Magn. Reson. Chem.*, **34**, S156–S176.
37. Nuoffer,C. and Balch,W.E. (1994) Gtpases: multifunctional molecular switches regulating vesicular traffic. *Ann. Rev. Biochem.*, **63**, 949–990.
38. Takai,Y., Sasaki,T. and Matozaki,T. (2001) Small GTP-binding proteins. *Physiol. Rev.*, **81**, 153–208.
39. Shimizu,H., Donohue-Rolfe,A. and Homans,S.W. (1999) Derivation of the bound-state conformation of a ligand in a weakly aligned ligand–protein complex. *J. Am. Chem. Soc.*, **121**, 5815–5816.
40. Bolon,P.J., Al-Hashimi,H.M. and Prestegard,J.H. (1999) Residual dipolar coupling derived orientational constraints on geometry in a 53 kDa protein–ligand complex. *J. Mol. Biol.*, **293**, 107–115.
41. Al-Hashimi,H.M., Bolon,P.J. and Prestegard,J.H. (2000) Molecular symmetry as an aid to geometry determination in ligand protein complexes. *J. Magn. Reson.*, **142**, 153–158.
42. Jain,N.U., Noble,S. and Prestegard,J.H. (2003) Structural characterization of a mannose-binding protein–trimannoside complex using residual dipolar couplings. *J. Biomol. NMR*, **328**, 451–462.
43. Umemoto,K., Leffler,H., Venot,A., Valafar,H. and Prestegard,J.H. (2003) Conformational differences in liganded and unliganded states of Galectin-3. *Biochemistry*, **42**, 3688–3695.
44. Amor,J.C., Harrison,D.H., Kahn,R.A. and Ringe,D. (1994) Structure of the human ADP-ribosylation factor 1 complexed wtih GDP. *Nature*, **372**, 704–708.
45. Seidel,R.D., Amor,J.C., Kahn,R.A. and Prestegard,J.H. (2004) Conformational changes in human Arf1 on nucleotide exchange and deletion of membrane-binding elements. *J. Biol. Chem.*, **279**, 48307–48318.
46. Kishore,A.I. and Prestegard,J.H. (2003) Molecular orientation and conformation of phosphatidylinositides in membrane mimetics using variable angle sample spinning (VASS) NMR. *Biophys. J.*, **85**, 3848–3857.
47. Freyssingeas,E., Nallet,F. and Roux,D. (1996) Measurement of the membrane flexibility in lamellar and 'sponge' phases of the C12E5/ hexanol/water system. *Langmuir*, **12**, 6028–6035.
48. Jonstromer,M. and Strey,R. (1992) Nonionic bilayers in dilute solutions: effect of additives. *J. Phys. Chem.*, **96**, 5993–6000.
49. Ruckert,M. and Otting,G. (2000) Alignment of biological macromolecules in novel non-ionic liquid crystalline media for NMR experiments. *J. Am. Chem. Soc.*, **122**, 7793–7797.
50. Maurer,T. and Kalbitzer,H.R. (1996) Indirect referencing of ^{31}P and ^{19}F NMR Spectra. *J. Magn. Res. Ser. B*, **113**, 177–178.
51. Wishart,D.S., Bigam,C.G., Yao,J., Abildgaard,F., Dyson,H.J., Oldfield,E., Markley,J.L. and Sykes,B.D. (1995) ^{1}H, ^{13}C and ^{15}N chemical-shift referencing in biomolecular NMR. *J. Biomol. NMR*, **6**, 135–140.
52. Delaglio,F., Grzesiek,S., Vuister,G.W., Zhu,G., Pfeifer,J. and Bax,A. (1995) NMRPipe: a multidimensional spectral processing system based on UNIX pipes. *J. Biomol. NMR*, **6**, 277–293.
53. Seidel,R.D., Amor,J.C., Kahn,R.A. and Prestegard,J.H. (2004) Structural perturbations in human ADP ribosylation factor-1 accompanying the binding of phosphatidylinositides. *Biochemistry*, **43**, 15393–15403.
54. Randazzo,P.A. (1997) Functional interaction of ADP-ribosylation factor 1 with phosphatidylinositol 4,5-bisphosphate. *J. Biol. Chem.*, **272**, 7688–7692.
55. Terui,T., Kahn,R.A. and Randazzo,P.A. (1994) Effects of acid phospholipids on nucleotide exchange properties of ADP-ribosylation factor 1. Evidence for specific interaction with phosphatidylinositol 4,5-bisphosphate. *J. Biol. Chem.*, **269**, 28130–28135.
56. Lundberg,P., Harmsen,E., Ho,C. and Vogel,H.J. (1990) Nuclear magnetic resonance studies of cellular metabolism. *Anal. Biochem.*, **191**, 193–222.
57. Rothman,D.L., Magnusson,I., Katz,L.D., Shulman,R.G. and Shulman,G.I. (1991) Quantitation of hepatic glycogenolysis and gluconeogenesis in fasting humans with ^{13}C NMR. *Science*, **254**, 573–576.
58. Szyperski,T. (1998) ^{13}C-NMR, MS and metabolic flux balancing in biotechnology research. *Q. Rev. Biophys.*, **31**, 41–106.
59. Voet,D. and Voet,J.G. (1995) *Biochemistry, 2nd edn.* John Wiley & Sons, Inc., NY.
60. Wood,T. (1985) *The Pentose Phosphate Pathway.* Academic Press, Inc., Orlando.
61. Magnusson,I., Chandramouli,V., Schumann,W.C., Kumaran,K., Wahren,J. and Landau,B.R. (1988) Pentose pathway in human liver. *Proc. Natl Acad. Sci. USA*, **85**, 4682–4685.
62. Kunnecke,B. and Seelig,J. (1991) Glycogen metabolism as detected by *in vivo* and *in vitro* ^{13}C-NMR spectroscopy using [1,2-^{13}C2]glucose as substrate. *Biochim. Biophys. Acta*, **1095**, 103–113.
63. Castellani,F., van Rossum,B.J., Diehl,A., Rehbein,K. and Oschkinat,H. (2003) Determination of solid-state NMR structures of proteins by means of three-dimensional ^{15}N–^{13}C–^{13}C dipolar correlation spectroscopy and chemical shift analysis. *Biochemistry*, **42**, 11476–11483.
64. Stueber,D. and Grant,D.M. (2002) ^{13}C and ^{15}N chemical shift tensors in adenosine, guanosine dihydrate, 2′-deoxythymidine, and cytidine. *J. Am. Chem. Soc.*, **124**, 10539–10551.